

STRONGLY TAPERED UNDULATOR DESIGN FOR HIGH EFFICIENCY AND HIGH GAIN AMPLIFICATION AT 266 nm

Youna Park, Nick Sudar, Pietro Musumeci, UCLA, Los Angeles, CA 90095, USA
 Yine Sun, Alexander Zholents, ANL, Argonne, IL 60439, USA
 Alex Murokh, RadiaBeam, Los Angeles, CA 90404, USA
 David Bruhwiler, Chris Hall, Stephen Webb, RadiaSoft, Boulder, CO 80301, USA

Abstract

Tapering Enhanced Stimulated Superradiant Amplification (TESSA) is a scheme developed at UCLA to increase efficiency of Free Electron Laser (FEL) light to above 10% using intense seed pulses, strongly tapered undulators and prebunched electron beams. Initial results validating this method have already been obtained at 10- μ m wavelength at Brookhaven National Laboratory. In this paper we will discuss the design of an experiment to demonstrate the TESSA scheme at high gain and shorter wavelength (266 nm) using the Linac Extension Area (LEA) beamline at the Advanced Photon Source of Argonne National Laboratory (ANL) to obtain conversion efficiencies around 10% depending on the length of the tapered undulator (up to 4m).

INTRODUCTION

X-ray Free Electron Lasers (FEL) have revolutionized the trajectory of science opening the door to the direct study at atomic spatial and temporal scales of fundamental systems such as chemical bond formation, motion of electrons through materials, 3D images of proteins and many more [1]. In high gain FELs the efficiency of electron beam energy conversion into radiation is typically limited to less than 1% due to the saturation effect [2]. Tapering the undulator parameters offers an opportunity to extend the interaction beyond initial saturation [3], and has been shown to provide a boost in efficiency. The Tapering Enhanced Stimulated Superradiant Amplification (TESSA) [4] method using a strongly tapered undulator an intense input seed laser and prebunched electron beams to greatly increase the conversion efficiency has been validated at Brookhaven National Laboratory (BNL) for 10 μ m wavelength and 50 cm strongly tapered undulator demonstrating efficiency greater than 35% [5].

In this paper we discuss the design of an experiment where we will demonstrate TESSA at shorter wavelength (266 nm) using the higher energy electron beam at APS linac. This experiment, which we will refer to as TESSA-266, will start with GW-level seed power and demonstrate 30 MeV/m energy exchange rates leading to a final gain of a factor of 10 in laser power. For this experiment we will use the APS injector linac at Argonne National Laboratory (ANL) which has been recently upgraded with an LCLS style photoinjector and can deliver high brightness beams to an experimental beamline where we will install the tapered undulator.

In an FEL, resonant wavelength of interaction is defined as $\lambda = (\lambda_w/2\gamma^2)(1 + K^2)$, where γ is particle energy, K undulator vector potential, and λ_w undulator period.

Table 1: Simulation Parameters of APS Linac

Electron beam energy	375 MeV
Peak current	1 kA
Seed power	< 1 GW
Normalized emittance	2 μ m

The particle energy evolution can be written as $d\gamma^2/dz = -2kK_l K \sin(\Psi_r)$ where $K_l = eE_0/km_e c^2$ laser vector potential and E_0 electric field of radiation, K undulator vector potential, and Ψ_r resonant phase. By taking the derivative of the resonance condition and using energy evolution equation we obtain the tapering equation for the normalized magnetic field amplitude along the helical undulator:

$$\frac{dK}{dz} = \frac{(1 + K^2)(dk_w/dz)}{2Kk_w} - k_w K_l \sin \Psi_r. \quad (1)$$

While period tapering is a possibility, we will limit this initial discussion to a constant period case (i.e. $dk_w/dz = 0$) and allow the gap inside the undulator to change to modify the magnetic field amplitude.

MAGNETIC SIMULATION OF UNDULATOR

Undulator Period vs. Beam Clearance

We used Radia to find the peak magnetic field for different undulator periods and gap at the center of the undulator. Figure 1 shows how the undulator vector potential K would vary as we change the undulator period. Where the resonance

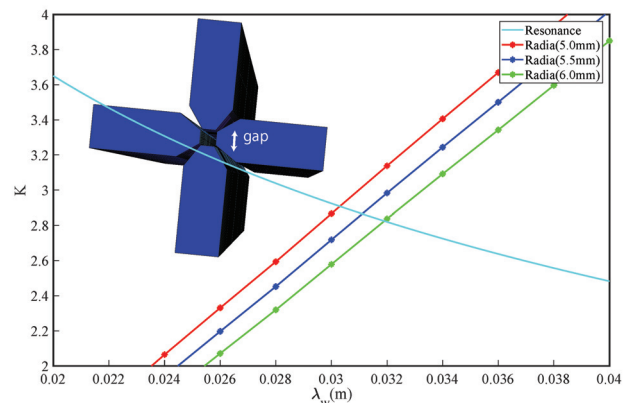


Figure 1: Undulator vector potential vs. undulator period for different gaps plotted with resonance condition.

Content from this work may be used under the terms of the CC BY 3.0 licence (© 2018). Any distribution of this work must maintain attribution to the author(s), title of the work, publisher, and DOI.

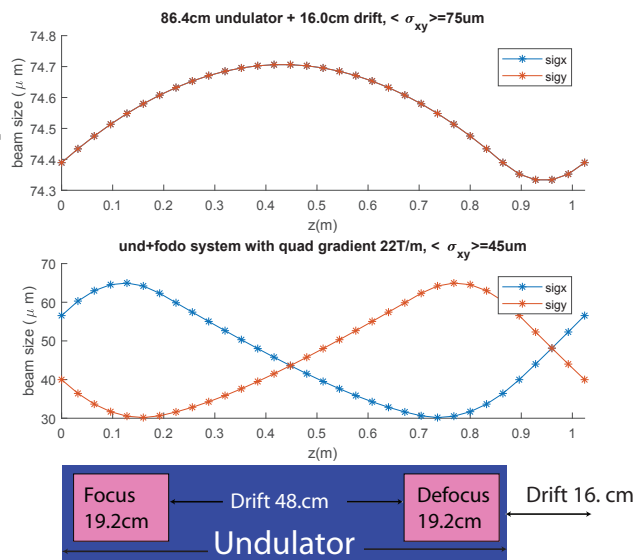


Figure 2: Top: Beam spot size for 3.2-cm period and 86.4-cm long undulator with 16-cm drift. bottom: Beam spot size for 3.2-cm period undulator with a diagram of FODO setup.

line (cyan) meets the data shows the period at resonance for different gaps of 5.0 mm, 5.5 mm, and 6.0 mm. As the thickness of the undulator and the magnet holder clearance required to assemble the undulator were not modified in the simulations, this should be considered as a rough estimate of possible undulator period. The 3.0-cm period is the bare minimum with the beam clearance of 5.1 mm (at the center of the undulator) and holder clearance of 3 mm (between the sides of undulator). We consequently decided that the best undulator period would be 3.2 cm.

The beam sizes matched to the undulator natural focusing beta-function for the period range of 3 cm–3.2 cm for 1-m long undulator were as large as 70 μm to 74 μm . Figure 2 shows that matched beam size for a 86.4 cm long undulator section followed by 16 cm drift was 74 μm with average beam size of 75 μm . This beam size would be relatively large compared to radiation spot size which will be around 100–120 μm depending on Rayleigh length and waist position and is not optimal for extraction efficiency. We consequently decided to look into installing quadrupoles around the undulator as in Figure 2 and 3 to decrease the electron beam sizes.

Quadrupole Design

Although placing quadrupoles compromises thickness of the undulator and consequently requires slightly longer period we found that the difference between the two magnetic undulator period designs was not significant (less than 1–2 mm) when considering the beam and the holder clearance so we decided that it is worthwhile to implement strong focusing in the undulator design. Figure 3 shows our preliminary undulator design of 3.2 cm period with beam clearance of 6 mm at the center and holder clearance of 4 mm around

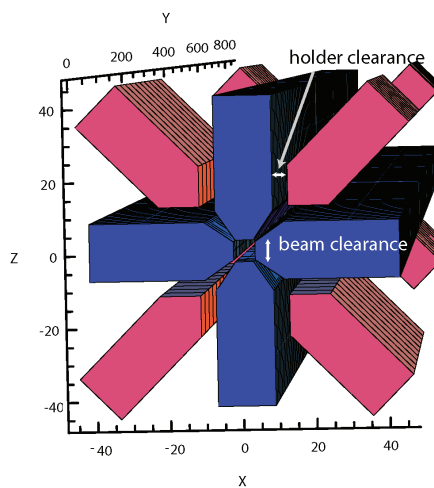


Figure 3: Radia simulation of undulator + quadrupole design for 3.2-cm undulator and 22-T/m quadrupole gradient. Blue = undulator, Red = quadrupoles. The tick marks are in 0.1-mm scale.

the sides of undulator and quadrupoles. This design gives maximum quadrupole gradient of 22 T/m which decreased average beam size to 45 μm (Figure 2). In principle it would be possible to further decrease the holder clearance around the magnets and increase overall focus and radiation power with custom design of magnets.

We studied the dynamics in the resultant FODO lattice to optimize beam size and power output given undulator period of 3.2 cm and maximum quadrupole gradient of 22 T/m. We simulated the simplest FODO system with focusing quadrupole, drift, and defocusing quadrupole to be placed inside the undulator. We varied lengths and gradients of the quadrupoles as both factors affect overall focusing strength, transverse electron propagation, and power output. Depending on the length of the undulator section it was possible to reduce average beam size upto 43 μm with quadrupole gradient of 22 T/m for undulator length of 64 cm. A more conservative design uses a 86.4 cm undulator which had greater power output due to the longer length. This 86.4 cm undulator and 16 cm drift system will have focusing and defocusing quadrupole lengths of 19.2 cm, 48.0 cm in between the two quadrupoles, and drift length of 16 cm between each undulator sections, and the system will have average beam size of 45 μm (Figure 2).

GIT SIMULATION OF 3.2-cm UNDULATOR

The beam energy is 375 MeV with a peak current of 1 kA, corresponding to 375 GW peak beam power. With approximately 10% efficiency, the peak power of the TESSA amplifier will be 20-40 GW, so that there will be considerable amount of change in the normalized field amplitude K_l along the undulator.

The system will operate in the TESSA high-gain regime. In order to optimize the tapering we used Genesis Informed

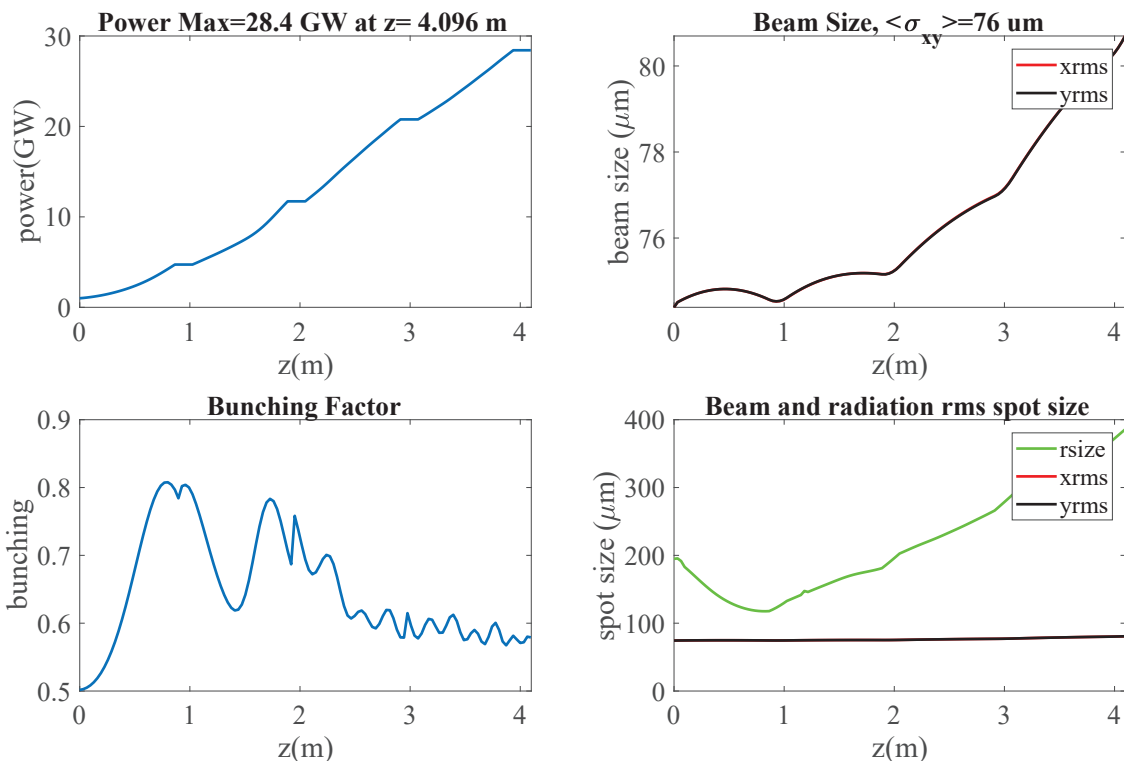


Figure 4: Power, Beam sizes, and bunching factor plots for four undulator sections of 86-cm undulator and 16-cm drift without quadrupoles.

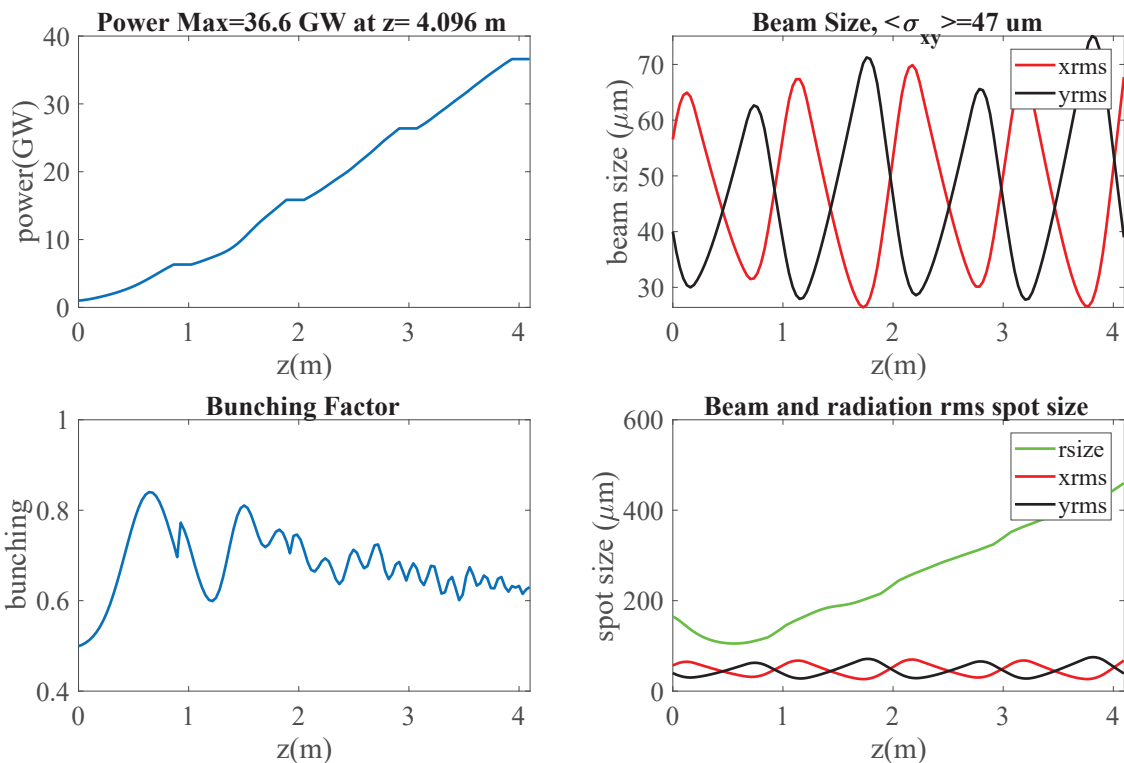


Figure 5: Power, Beam sizes, and bunching factor plots for four undulator sections of 86-cm undulator and 16-cm drift with quadrupoles.

Content from this work may be used under the terms of the CC BY 3.0 license (© 2018). Any distribution of this work must maintain attribution to the author(s), title of the work, publisher, and DOI.

Table 2: Simulation Parameters of Undulator

Simulation parameters of undulator	
Undulator Period	3.2 cm
Undulator gap	6 mm
Number of modules	4
Module length	4.096 m
Simulation results for undulator without FODO	
RMS beam size	76 μm
Power output	28.4 GW
Efficiency	7.6%
Simulation results for undulator with FODO	
RMS beam size	47 μm
Power output	36.6 GW
Efficiency	9.8 %

Tapering method where Genesis is called at each undulator period to simulate particle and radiation beam evolution and the tapering is varied following Equation (1) for the next period.

GIT Simulation of Undulator without Quadrupoles

Using GIT we simulated four sections 86.4-cm long undulators with 3.2-cm period. Figure (4) shows the average beam size of 76 μm and a final radiation power of 28.4 GW with an efficiency of 7.6%. For these simulations we assumed an initial bunching factor of 0.5 determined by a prebuncher with 4-cm-period undulator and a magnetic chicane located 52 cm before the entrance of the tapered undulator. The beam size slightly increases throughout longitudinal propagation due to the variation of K along the undulator.

GIT Simulation Undulator with Quadrupoles

For four sections of 86-cm undulators with FODO system of 19.2-cm long, 22-T/m gradient quadrupoles, 48.0-cm drift between the quadrupoles, and 16-cm drift between the undulators (Figure 2), we obtained average beam size of 47 μm and the final power output is 36.6 GW (Figure 5). The conversion efficiency of the system is 9.8%.

CONCLUSIONS

We show by 3D Genesis simulation that the TESSA-266 experiment could achieve an extraction efficiency of 7.6% without using strong focusing in the undulator and 9.8% with quadrupoles. This will be an order of magnitude improvement from the previous record values of efficiency at UV wavelengths [2]. The improvement has the potential for breakthrough impact in research areas such as materials synthesis, lithography, and nano-engineering where short wavelengths FELs are used [6]. The experiment will be the first time to demonstrate TESSA design at high regime taking advantage of strong focusing in the undulator.

ACKNOWLEDGMENT

This work has been supported by SBIR award DE-SC0017102.

REFERENCES

- [1] C. Bostedt *et al.*, "Linac coherent light source: The first five years," *Rev. Mod. Phys.*, vol. 88, p. 015007, 2016. Available: <https://link.aps.org/doi/10.1103/RevModPhys.88.015007>
- [2] D. Douglas *et al.*, "High average power uv free electron laser experiments at jlab," in *Proceedings of IPAC'12*, New Orleans, LA, USA, paper WEYB03.
- [3] N. Kroll, P. Morton, and M. Rosenbluth, "Free-electron lasers with variable parameter wigglers," *IEEE Journal of Quantum Electronics*, vol. 17, no. 8, pp. 1436–1468, 1981.
- [4] J. Duris, A. Murokh, and P. Musumeci, "Tapering enhanced stimulated superradiant amplification," *New Journal of Physics*, vol. 17, no. 6, p. 063036, 2015. Available: <http://stacks.iop.org/1367-2630/17/i=6/a=063036>.
- [5] N. Sudar *et al.*, "High efficiency energy extraction from a relativistic electron beam in a strongly tapered undulator," *Phys. Rev. Lett.*, vol. 117, p. 174801, 2016. Available: <https://link.aps.org/doi/10.1103/PhysRevLett.117.174801>.
- [6] E. R. Hosler, O. R. Wood, and W. A. Barletta, "Free-electron laser emission architecture impact on EUV lithography," *Proc. SPIE*, vol. 10143, pp. 101 431M–101 431M–12, 2017. Available: <http://dx.doi.org/10.1117/12.2260452>.